Polymer 50 (2009) 6083–6090

Contents lists available at ScienceDirect

Polymer

journal homepage: www.elsevier.com/locate/polymer

Heterogeneous structure of poly(glycolic acid) fiber studied with differential scanning calorimeter, X-ray diffraction, solid-state NMR and molecular dynamic simulation

Sokei Sekine [a,b], Kazuo Yamauchi [a], Akihiro Aoki [a], Tetsuo Asakura [a,*]

[a] Department of Biotechnology, Tokyo University of Agriculture and Technology, Koganei, Tokyo 184-8588, Japan
[b] Mitsui Chemical Analysis & Consulting Service, Inc., 580-32, Nagaura, Sodegaura 299-0265, Japan

ARTICLE INFO

Article history:
Received 10 July 2009
Received in revised form
7 October 2009
Accepted 19 October 2009
Available online 24 October 2009

Keywords:
Poly(glycolic acid)
Solid-state 13C NMR
Molecular dynamic simulation

ABSTRACT

The heterogeneous structures of poly(glycolic acid) (PGA) fibers which have been used as bio-degradable suture were studied by differential scanning calorimeter (DSC),X-ray diffraction and ^{13}C solid state NMR. The ^{13}C cross polarization NMR spectra without magic angle spinning of the stretched fibers observed by changing the angle between the fiber axis and the magnetic field clearly showed the heterogeneous structures which consist of three components; well-oriented, poorly-oriented and isotropic amorphous components. The local structure, distribution of the fiber axis and fraction of each component were determined quantitatively. Change in the heterogeneous structure by changing the stretching method in the sample preparation and by changing the stretching ratio was also monitored. The X-ray diffraction data of the fibers are in good agreement with the ^{13}C CP NMR data. Change in the heterogeneous structures correlate with change in the thermal properties observed by DSC method. The molecular dynamic simulation showed the generation of trans conformation of PGA chain and also change in the fraction of other conformations by stretching, which supports the experimental results obtained above and gives additional structural information.

1. Introduction

A semi-crystalline biodegradable polyester, Poly(glycolic acid)(PGA) [1–5] has been successfully used as suture materials after stretching the amorphous fiber. However, the main disadvantage of PGA for sutures is its high stiffness and therefore the polymer is processed in a multi-filament form to increase flexibility. In addition, the physical properties and related structures change largely by the processing condition such as stretching.

Chatani et al. [6] determined the crystal structure of stretched PGA fiber by X-ray diffraction method. The dimensions of the orthorhombic unit cell were reported to be $a = 5.22$ Å, $b = 6.19$ Å and c (fiber axis) $= 7.02$ Å. Two PGA chains with planar zig-zag conformation passing through the unit cell permit tight molecular-packing and close approach of the ester groups. However, the stretched PGA fibers are generally heterogeneous and therefore it is necessary to obtain more structural and dynamical information for such a heterogeneous sample which is closely related with the physical properties.

The solid-state NMR has been used for structural and dynamical studies of PGA. Sobczac et al. [7] used ^{13}C CP/MAS NMR to study phase structure and morphology of PGA sutures (Dexon). De Oca et al. [8] studied dynamics of un-stretched isotropic and highly-stretched PGA fibers by second-moment analysis of ^{1}H NMR signal and spin-lattice relaxation time, T_1 analysis by solid-state ^{1}H pulse NMR. They also studied theoretical modeling to explain the elastic behavior of PGA crystals [9]. The tensile modulus is higher along the fiber axis than the other directions. There is a good correction between the experimental modulus (294 GPa) and the theoretical predictions. However, the glass transition temperature, T_g determined experimentally is higher than the T_g value predicted theoretically. They speculated that such a higher shift of T_g is due to the existence of "oriented amorphous component".

We also studied the structure and dynamics of as-spun and stretched PGA fibers by solid echo ^{1}H NMR and WAXD methods [10]. The observed WAXD patterns of highly-stretched fibers showed sharp diffraction peaks from which the crystallinities of stretched fibers with the stretching ratios of 2.5, 2.8 and 3.2 were determined to be 0.50, 0.51 and 0.52, respectively. However, the

* Corresponding author. Tel.: +81 42 383 7733; fax: +81 42 388 7025.
E-mail address: asakura@cc.tuat.ac.jp (T. Asakura).

0032-3861/$ – see front matter © 2009 Elsevier Ltd. All rights reserved.
doi:10.1016/j.polymer.2009.10.040

observation of the ^{1}H spin–spin relaxation time (T_2) of these stretched fibers, showed quite different tendencies. The fractions of the "hard" component for the stretched PGA fibers with the stretching ratios of 2.5 and 3.1 were determined to be 0.62 and 0.93, respectively, at 120 °C, from the deconvolution of the observed ^{1}H FID signals. Thus, the picture of the heterogeneous structures is different depending on the analytical methods which indicate what kinds of structures are reflected in the different analytical methods.

The ^{13}C CP/MAS NMR has been frequently used for study heterogeneous polymer structure from the chemical shifts and line shape analyses including several relaxation time observations. However, MAS techniques sometimes delete important structural information instead of peak resolution and intensity enhancements. Thus, ^{13}C CP NMR observation in oriented and non-oriented samples without MAS spinning is sometimes effective for the ^{13}C carbon such as carbonyl carbon with large chemical shift anisotropies. Actually, we successfully applied ^{13}C CP NMR without MAS spinning to study the heterogeneous structures of *Bombyx mori* and *Samia cynthia ricini* silk fibers [11–16], and also stretched synthetic polymers such as poly(ethylene terephthalate) [17], poly(L-lactic acid) [18] and ply(ε-caprolacton) [19]. Importantly, such a ^{13}C CP NMR spectrum has been obtained as a function of the angle between the fiber axis and external magnetic field, which gives detailed information on the heterogeneous structures by analyzing the observed spectra on the basis of orientation-dependent spin interaction tensors.

In this paper, the heterogeneous structures of poly(glycolic acid) (PGA) fibers prepared by different stretching condition and stretching ratio will be studied by differential scanning calorimeter (DSC), X-ray diffraction and ^{13}C solid state NMR. Change in the conformation of PGA molecule by stretching will be also monitored theoretically by the molecular dynamics simulation.

2. Experimental part

2.1. Materials

PGA was synthesized by Mitsui Chemicals, Inc. and its molecular weight was determined to be about 2×10^5 using the gel permeation chromatography (GPC) method. PGA fibers were prepared at 230 °C from the molten state. After cooling them at room temperature, the amorphous fibers were stretched by two different methods. For case A (Pre-heated method); 10 cm of un-stretched PGA fibers were held on a tensile strength instrument for 1 min just above T_g of PGA and then, the fibers were stretched at the rate of 100 mm/min at 62 °C. The stretched samples were prepared to 1.5 and 3.5 times which were defined to be the ratio of stretched fiber length to original untreated fiber length. For case B (After-heated method); 10 cm of un-stretched PGA fibers were stretched at the rate of 100 mm/min. at 23 °C (below T_g) and then, the fibers were heated at 62 °C for 1 min. The stretching ratios were the same as those in case A. The tensile strength was measured at room temperature with an extension rate of 100 mm/min while keeping the gauge length, 100 mm. The heterogeneous structures of the stretched fibers prepared by these two methods are different even if the stretching ratio is the same.

2.2. DSC measurement

The DSC measurements were carried out with a Perkin–Elmer Pyris 1 instrument to observe T_g and T_m temperatures. To avoid a change of T_m of the PGA fiber sample by its shrinkage, the fibers were bound by a fine metal wire and coiled on the sample pan while keeping a strain of the fibers. The heating rate was 10 °C/min. T_g was determined from the mid-point of specific heat transition.

2.3. X-ray diffraction measurement

Wide-angle X-ray diffraction (WAXD) of the un-stretched and stretched PGA fibers was observed by a Rigaku RINT2500 X-ray instrument utilizing nickel-filtered CuK_α radiation (wave length $\lambda = 1.54$ Å) at room temperature. PGA fibers were rolled and mounted carefully to avoid further stretching of the samples on a holder.

2.4. Solid-state NMR

^{13}C solid state NMR experiments were performed at 23 °C using a Bruker AVANCE400 WB spectrometer at resonance frequencies of 100.6 MHz for ^{13}C nuclei. The ^{13}C CP/MAS NMR spectra were recorded under observation conditions, a CP contact time of 3 ms, a repetition time of 5 s, a spinning speed of 7 KHz and the numbers of scans were 4 k. The ^{13}C CP NMR spectra of the blocks of uniaxially stretched PGA fibers were also obtained under similar observation conditions without MAS spinning. In this observation, a home built probehead with a 1 cm square coil for ^{13}C observation with ^{1}H decoupling was used. The angle of the fiber axis and the magnetic field was changed. Typically, 12k scans were accumulated for each spectrum. The ^{13}C chemical shift tensors of the carbonyl carbons of these samples were obtained by fitting the line shape of amorphous PGA fibers [17]. The simulations of the angle-dependent ^{13}C CP NMR spectra on the basis of chemical shift anisotropies were performed by the least-square method [17–19].

2.5. Molecular dynamic simulation

The molecular dynamics (MD) and molecular mechanics (MM) calculations were carried out by using 'Material Studio 4.1 Discover' module (Accelrys Inc.). All of the simulations were performed by using pcff force field (Accelrys Inc.). The model of initial amorphous PGA structure before stretching was reproduced as follows. The 18 PGA chains with 20 polymerization degree and with all trans conformations were generated on the computer according to the crystal structure of stretched PGA fiber by X-ray diffraction method [6]. Then 2 Å was added to the distance of the inter-chains along *a* and *b* axes to produce amorphous state. The infinite bulk system of the infinite repeated polymer chains, periodic boundary condition, was set. Then, MD simulations were performed at 10,000 steps at 1000 °C under external shear stress of 0.3 GPa which was set parallel to the fiber axis, *c* axis. Then, additional MD simulation under equivalent hydrostatic pressure of 1.0 GPa and then annealing was performed. The amorphous PGA structure with density of 1.50 determined experimentally [20] for amorphous PGA sample was obtained. The stretching of such amorphous PGA chains was performed as follows. 4 Å was added to the original chain length of each chain selected from 18 chains and then MD simulation was performed at 50,000 steps (50 psec) at 100 °C under the fixed co-ordinates of the end atoms of the PGA molecule. The same process was repeated for 18 PGA chains. Then MM calculation was then performed to minimize the conformational energies. This process (adding each 4 Å to the end-to-end distance of the stretched PGA chain) was repeated and conformational distribution of the PGA chains was obtained under increase in the stretching ratio. Finally, the stretched PGA chains with stretching ratio from 1.0 to 1.91 for each 0.11 increase were obtained. The internal rotation angles of the C–C or C–O bonds of PGA molecules after MD and then MM calculations were plotted to examine conformational change by stretching.

3. Results and discussion

3.1. Glass transition and melting temperatures determined by DSC measurement

The difference in the thermal properties between two preparation methods, for cases A and B, was noted by DSC measurement (Fig. 1). The T_g was determined by the mid-height of the tangent line before and after specific heat transition. The example of the determination is shown for the PGA fiber with stretching ratio 1.5 times (case B (·····)). The T_g was determined to be 44.6 °C (×1.5) and 48.9 °C (×3.5) for case A, and 48.6 °C (×1.5) and 53.7 °C (×3.5) for case B.

As shown in Fig. 2, the melting temperature for case A was determined from the peak top to be 221.5 °C (×1.5) and 220.8 °C (×3.5), and for case B was 221.8 °C (×1.5) and 223.5 °C (×3.5). The T_g become higher with increasing the stretching ratio for both cases. The un-stretched PGA fiber was not crystallized and therefore the re-crystallization begun from 60 °C. The T_g of the stretched fiber samples prepared according to case B was about 4 °C higher than those of the samples prepared according to case A when the stretching ratio was the same. This difference in the T_g between the two cases seems due to the difference in the mobility of the amorphous region. The amorphous region of the stretched PGA fibers is more restricted for case B than for case A by orientation.

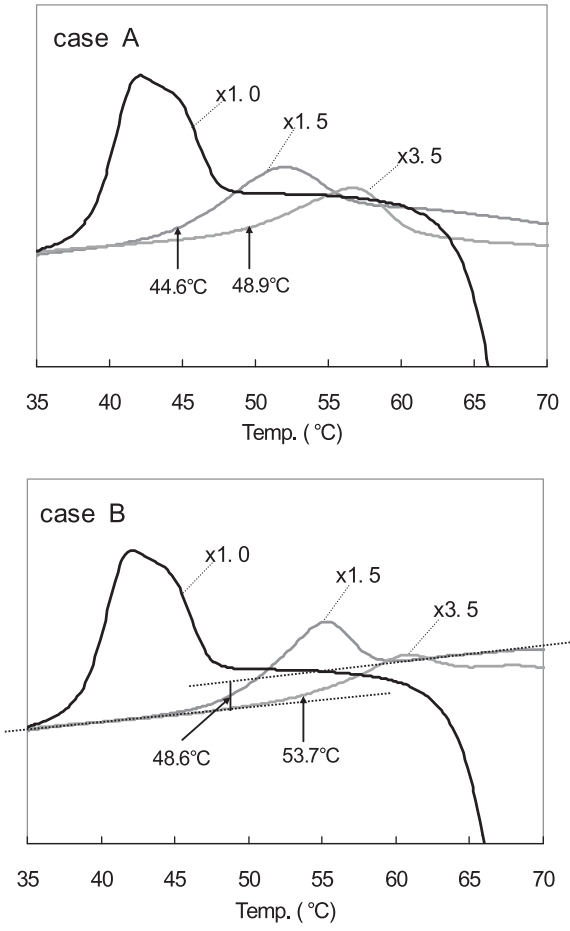

Fig. 1. The DSC results for determination of the glass transition temperature (T_g) by the mid-height of the tangent line before and after specific heat transition of the un-stretched, stretched PGA fibers with stretching ratios of 1.5 and 3.5 prepared with different methods, cases A and B. The tangent line (·····) of before and after specific heat transition and the height (———) of specific heat shift with stretching ratio 1.5 times, prepared by the case B method.

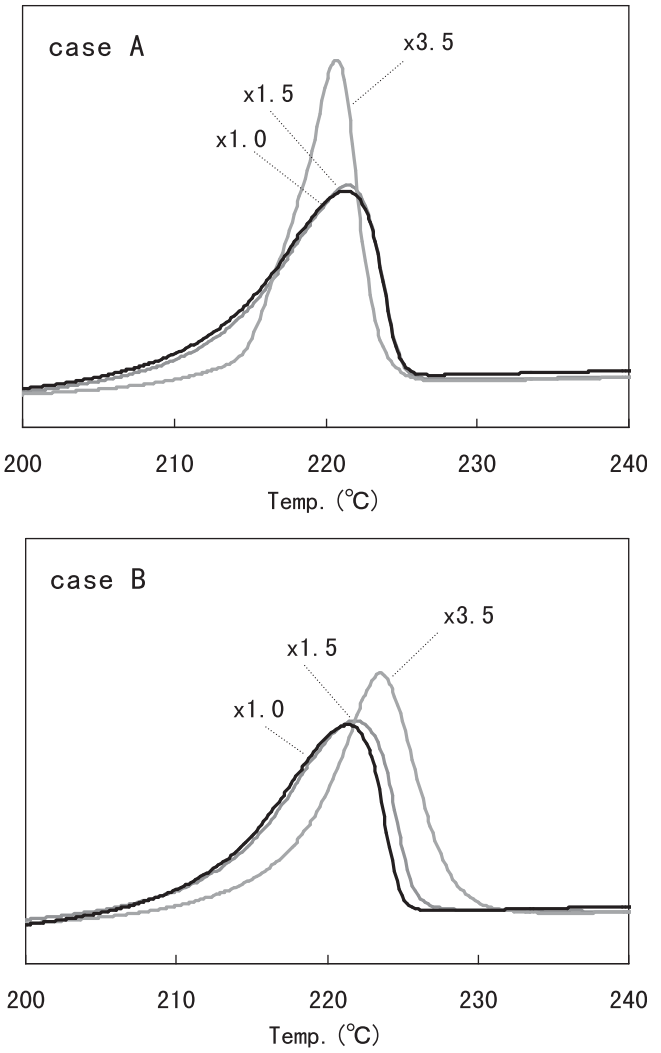

Fig. 2. The DSC results for determination of the melting temperature (T_m) of the un-stretched, stretched PGA fibers with stretching ratios of 1.5 and 3.5 prepared with different methods, cases A and B.

For example, the elevation in the melting temperature was also observed with stretching ratio 3.5 for case B. This comes from the entropy effect of molecular chain orientation.

According to the melting behavior study of Todoki et al. based on Zachmann's theory [21], the equilibrium melting point T_m^0 is given by

$$T_m^0 = \overline{\Delta H^0}/\overline{\Delta S^0}$$

where $\overline{\Delta H^0}$ and $\overline{\Delta S^0}$ are the melting mean value of enthalpy and entropy of fusion, respectively [22,23]. The enthalpy of melting ΔH^0 is assumed to be unchanged through the melting process and it is the same as the mean value $\overline{\Delta H^0}$, the melting temperature T_m is dependent on the entropy of melting ΔS^0. This DSC measurement was performed by keeping a strain of the fibers prevented from shrinking during melting process. If the molecular orientation was remained after melting, the ΔS^0 should be smaller than $\overline{\Delta S^0}$, and then T_m would be shift to higher temperature [23,24].

The melting behavior study of the stretched nylon 6 by Todoki et al. shows the higher T_m shift with increasing stretching ratio for samples stretched at 55 °C, 222.0 °C (×1.0), 223.5 °C (×2.5), 225.2 °C (×3.0), 229.1 °C (×4.0), 231.2 °C (×5.0), and the measurement was performed by keeping a strain of the fibers

which were prevented from shrinking during the melting process [23,24]. Our measurement was operated with the same as their operating method. The melting point of the PGA fiber with stretching ratio (×3.5) was about 2 °C higher than that of the stretching ratio (×1.5) for case B. The melting temperature of case A was not changed with the stretching ratio (×1.5) and (×3.5), and was the same as (×1.5) for case B. The DSC data shows that the entropy of case B was smaller than for case A with a stretching ratio of 3.5. It was considered that the molecular chain of case B was relatively oriented and restricted by stretching. The reason was thought to be that the melting temperature of case B with a stretching ratio of 3.5 was shifted to a higher temperature, and case B was highly oriented regarding the PGA fiber axis of crystalline and amorphous regions when stretched compared to case A. In order to clarify the difference of DSC data by stretching method, WAXD, ^{13}C CP/MAS NMR and ^{13}C CP NMR were used for analyses of the heterogeneous structure.

3.2. Structure of PGA fibers characterized by wide-angle X-ray diffraction (WAXD) pattern

Fig. 3 shows WAXD patterns of the stretched PGA fibers with stretching ratios of 1.5 and 3.5 prepared with different methods, cases A and B, together with an un-stretched sample. The un-stretched PGA fiber with a hollow X-ray diffraction pattern indicates an amorphous sample. The reflections, (1 1 0) and (0 2 0) marked in the Figure were observed with stretching ratios of 1.5 and 3.5 [6]. The crystallinities of the stretched fibers with stretching ratios of 1.5 and 3.5 were determined to be 0.34 and 0.36 for case A, and 0.33 and 0.37 for case B. Thus, there are no significant differences between cases A and B. In addition, only small increases in the crystallinities were observed for both cases by increasing stretching ratio. However, an increase in the orientation of the crystalline domain by stretching is clear for both cases. The degrees of orientation obtained from (0 2 0) reflection were determined to be 0.76 (×1.5) and 0.92 (×3.5) for case A, and 0.82 (×1.5) and 0.95 (×3.5) for case B, respectively. Thus, the orientation of the crystalline becomes higher with increasing the stretching ratio, and case B is highly oriented compared to case A with each stretching ratio. The reflection width of case B tends to be smaller than that of case A.

3.3 ^{13}C CP/MAS NMR spectra

Fig. 4 shows expanded CH_2 and C=O peaks in the ^{13}C CP/MAS NMR spectra of un-stretched and uniaxially stretched PGA fibers with stretching ratios of 1.5 and 3.5 times (case B). The spectra are very simple and only these two peaks were observed, which is suitable for the angle-dependent NMR experiments performed here because of no peak overlapping in the ^{13}C CP NMR. The CH_2 peak was much broader for the former sample, while the asymmetric peak was observed for uniaxially stretched PGA fibers. The peak tends to be slightly broader when the stretching ratio is 3.5 times compared with the sample with 1.5 times. The highest peak of 62.5 ppm at the lower field is easily assigned to all trans conformation and the shoulder at the higher field at around 61 ppm to amorphous peak. Actually, the chemical shift of the shoulder at the higher field of the asymmetric peak agrees with that of the broad main peak of the un-stretched PGA fiber. In the carbonyl region, the peak width becomes considerably narrower when the PGA fiber was stretched. Similar to the case of CH_2 peak, the carbonyl peak tends to be slightly broader when the stretching ratio is 3.5 times compared with the sample with 1.5 times.

3.4. ^{13}C CP NMR spectra of PGA fiber blocks as a function of the angle between the fiber axis and external magnetic field

Both CH_2 and carbonyl carbons of the stretched PGA fibers show the angle-dependent spectra, but the chemical shift anisotropy is considerably larger for the carbonyl carbon compared with the CH_2 carbon. Such a carbonyl carbon is suitable for detailed structural analysis on the basis of orientation-dependent spin interaction tensors and therefore only carbonyl carbon was used for the analysis in this paper.

At first, the ^{13}C CP NMR spectra of un-stretched PGA fiber blocks after setting the aligned fiber axis perpendicular and parallel to the magnetic field were observed (Fig. 5). The chemical shift tensor values of the carbonyl carbon were determined by the spectral simulation of the isotropic amorphous pattern as $\sigma_{11} = 112.7$ ppm, $\sigma_{22} = 130.4$ ppm and $\sigma_{33} = 260.5$ ppm. Thus, the isotropic chemical shift, σ_{iso} of the carbonyl peak of the amorphous PGA fiber was calculated as 167.7 ppm which coincides with the corresponding value, 168 ppm observed from the ^{13}C CP/MAS NMR spectrum of the amorphous PGA sample in Fig. 4. There is no significant difference between these two spectra of the un-stretched PGA fiber blocks, indicating absence of oriented components in the sample. Thus, the un-stretched fiber takes a completely disordered structure.

On the other hand, the ^{13}C CP NMR spectra of the block of the stretched PGA fibers change largely depending on the angle, β_L between the fiber axis and magnetic field. As an example, Fig. 6 shows the carbonyl carbon spectra of the block of PGA fibers with the stretching ratio of 3.5 (case B) as a function of the angle, β_L (0°, 30°, 45°, 65° and 80°) together with the peak simulation. The angle dependent spectra mean the presence of oriented components in the sample. However, it is also noted that there are an angle-independent component which is always observed after changing the angle, β_L.

3.5. Structural analyses of carbonyl carbon peaks of stretched PGA fibers

The five angle-dependent spectra in Fig. 6 were tried to simulate according to the analytical methods reported previously [11–19]. At first, the simulation was performed using the chemical shift tensors by assuming two kinds of components in the stretched PGA fibers, that is, only angle-dependent and angle–independent components. However, the agreement between the observed and simulated spectra was very poor (data not shown). Therefore the simulation was performed by assuming three components, that is, well-oriented (·····) and poorly-oriented (·····) components which are angle-dependent together with the angle-independent (——) component. As shown in Fig. 6, the observed spectra can be produced by the simulated spectra and thus, we could determine the structural parameters of these heterogeneous PGA fibers with a stretching ratio of 3.5. The relatively sharper peaks are the well-oriented component and the broader one is the poorly-oriented component. The presence of two kinds of angle-dependent components has also been reported for stretched poly(ethylene terephthalate), poly(L-lactic acid) and ply(ε-caprolacton) films [17–19].

The simulated results of this sample and other stretched PGA fibers in the angle-dependent ^{13}C CP NMR spectra are summarized in Table 1. The definitions of the angles, α_F and β_F and p values were described in the previous papers [11–19]. The angle, α_F was assumed to be 90° by reference of the analysis of stretched poly(ethylene terephthalate) film. The angle β_F and the standard deviation of the assumed Gaussian distribution around β_L, p, were changed for two oriented components; the well-oriented and the poorly oriented ones under the fixed line broadening factor, 6 Hz. In addition, the fractions of these two components together with the amorphous component were changed simultaneously.

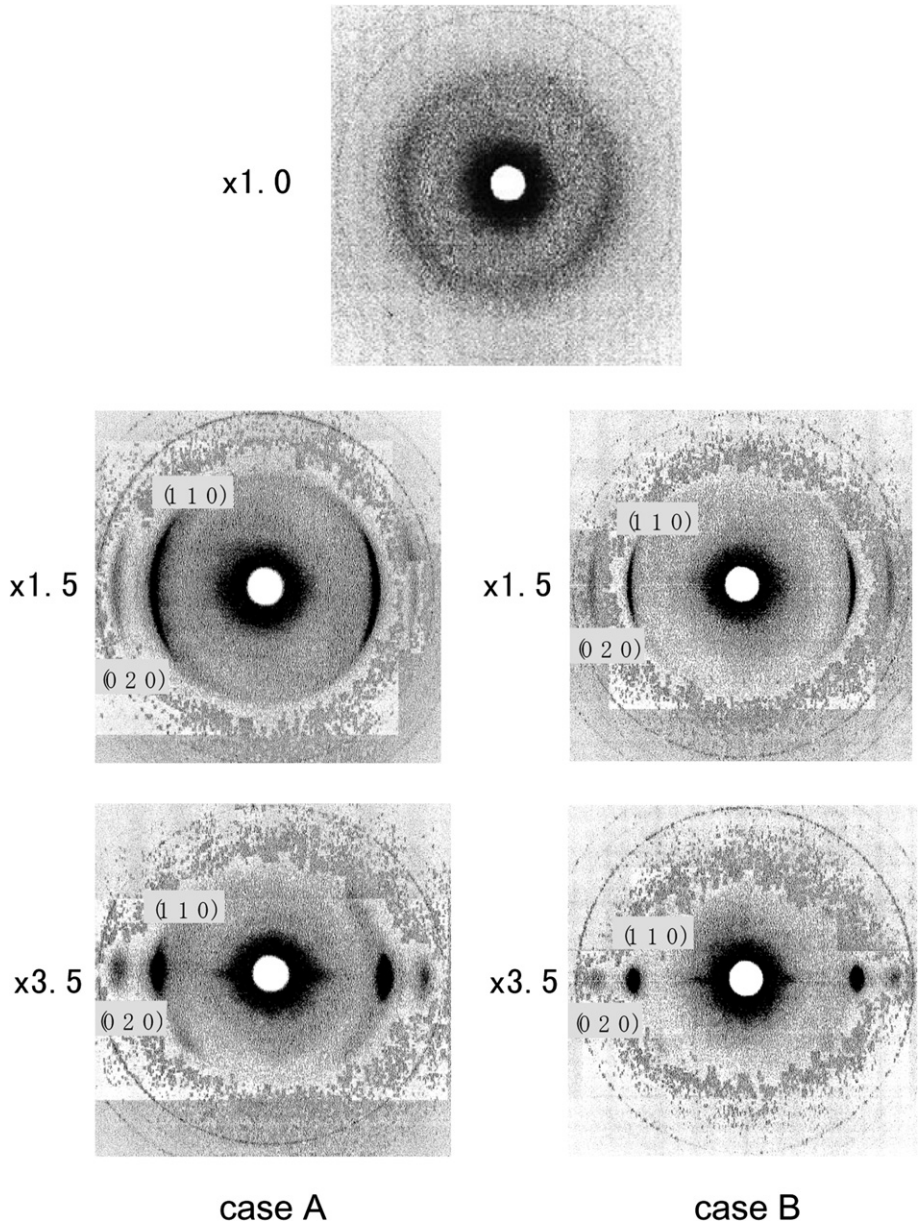

Fig. 3. X-ray diffraction patterns of the un-stretched, stretched PGA fibers with stretching ratios of 1.5 and 3.5 prepared with different methods, cases A and B.

We checked the change in the fraction of each component of the heterogeneous structure by stretching treatment. In the case of A, by 1.5 times stretching of the un-stretching PGA fiber, the structural change occurred from amorphous component to well-oriented component (15%) and to poorly-oriented component, 22%. On the other hand, for 3.5 times stretching, increase in the fraction of the structural change from the amorphous region to well-oriented component (30%) occurred exclusively and the fraction of the

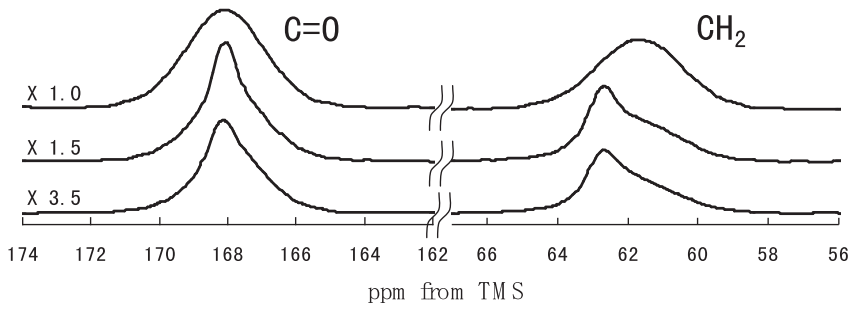

Fig. 4. The expanded CH_2 and C=O peaks in the ^{13}C CP/MAS NMR spectra of un-stretched and uniaxially stretched PGA fibers with stretching ratios of 1.5 and 3.5 times (case B).

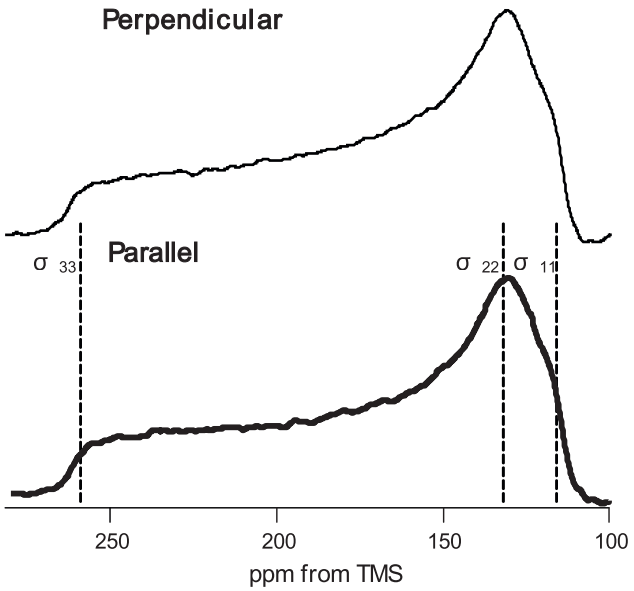

Fig. 5. ^{13}C CP NMR spectra of un-stretched PGA fiber block after setting the aligned fiber axis perpendicular and parallel to the magnetic field.

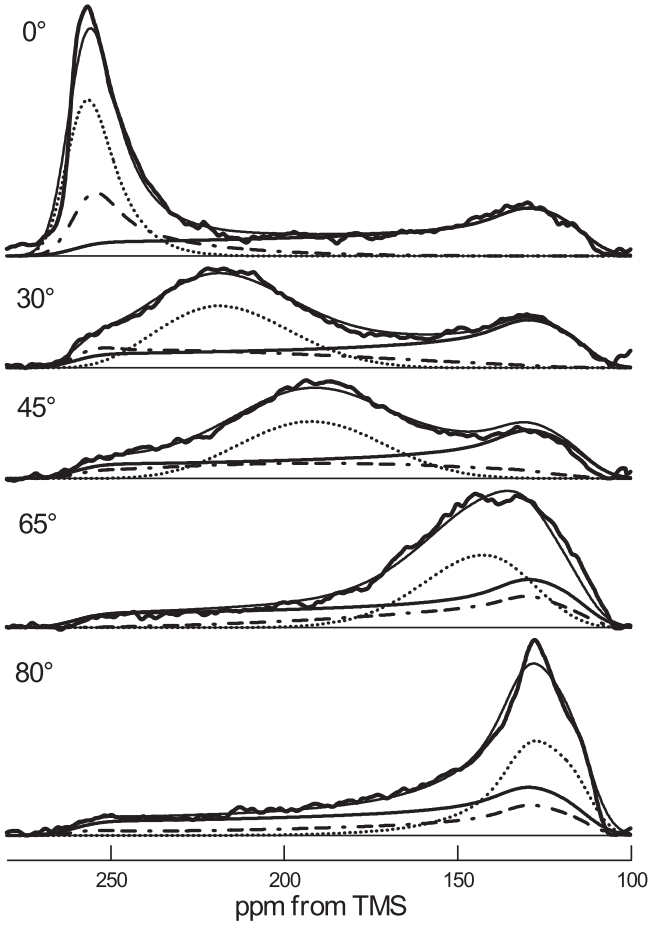

Fig. 6. ^{13}C CP NMR carbonyl spectra of the stretched PGA fibers block with the stretching ratio of 3.5 (case B) by changing the angle, β_L (0°, 30°, 45°, 65° and 80°) between the fiber axis and magnetic field. The peak simulations were shown as described in the text in detail. The peak simulation was performed by assuming three components, 1: well-oriented (·····), 2: poorly-oriented (- - - - -) and amorphous component (———) on the basis of orientation-dependent spin interaction tensors.

poorly-oriented component (17%) does not increase or rather only slightly decreased.

In the case of B, a similar tendency was obtained compared with case A, but there are also different tendencies locally. For example, by 1.5 times stretching, the structural change from amorphous components to both well-oriented (15%) and poorly-oriented (27%) components occurs. The fraction of the poorly-oriented component is larger by 1.8 times than the fraction of the well-oriented component. However, for 3.5 times stretching, the fraction of the well-oriented (35%) component increases remarkably compared to the fraction of the poorly-oriented (21%) component. This means that the orientation in the PGA sample occurs largely for case B than for case A by large stretching treatment (×3.5) and the well-oriented PGA fiber can be obtained by case B. These data are in good agreement with the results by WAXD analyses, that is, the reflections were determined to be 0.76 (×1.5) and 0.92 (×3.5) for case A, and 0.82 (×1.5) and 0.95 (×3.5) for case B, respectively. The WAXD data show highly orientation in case B.

Here we will discuss the change in local structure including the orientation distribution of each component of the heterogeneous structure by stretching treatment. The angular-dependence ^{13}C CP NMR spectra of the stretched PGA fibers with stretched ratios, ×1.5 and ×3.5 show two oriented-components; $p_1 = 13$ with $\beta_F = 13°$ (×1.5) and $p_1 = 13$ with $\beta_F = 12°$ (×3.5) for the well-oriented component, and $p_2 = 22$ with $\beta_F = 30°$ (×1.5) and $p_2 = 18$ with $\beta_F = 25°$ (×3.5) for the poorly-oriented component for case A. On the other hand, the p_1 was 7 with $\beta_F = 5°$ (×1.5) and 6 with $\beta_F = 6°$ (×3.5) for the well-oriented component, and p_2 was 16 with $\beta_F = 17°$(×1.5) and 16 with $\beta_F = 16°$(×3.5) for the poorly-oriented component for case B. The smaller p values indicate a smaller distribution of the fiber axis and therefore both well-oriented and poorly-oriented components of the PGA fibers are relatively highly oriented for case B compared with case A. These data are also in agreement with the WAXD analyses, the differences are not only higher orientation in case B but also smaller reflection width for case B. These data show that PGA fibers are highly oriented for the fiber axis and the distribution of orientation is smaller in case B. However, even if the stretching ratio increases, the p value of each component does not change significantly. The fraction of the well-oriented component increases largely with increasing the stretching ratio for both cases.

From the ^{13}C CP NMR and WAXD analyses, the relationship between DSC data (T_g and T_m) and heterogeneous structure by different stretching methods is considered as following reasons. According to the ^{13}C CP NMR, the summation of well-oriented and poorly-oriented components in case B is larger than that for case A, the β_F and p factor is smaller in case B than for case A. These data show the highly oriented tendency in case B. Furthermore the summation of well-oriented and poorly oriented components is larger than the crystallinities determined from WAXD analyses. These data indicate that the orientation is not only crystalline but also amorphous. Thus, the T_g of the stretched fiber samples prepared according to case B was higher because of the amorphous regions oriented for fiber axis.

The melting point of the PGA fiber with stretching ratio (×3.5) was about 2 °C higher than that of stretching ratio (×1.5) for case B [23,24]. The melting temperature of case A was not changed with the stretching ratio (×1.5) and (×3.5), the same as (×1.5) with case B. This might be the reason why the T_m of case B with stretching ratio 3.5 shifted to a higher temperature, that is, the fibers in case B was highly oriented around the fiber axes of crystalline and amorphous regions by stretching which were obtained from ^{13}C CP

Table 1
Structural parameters of stretched PGA fibers determined by angle-dependent ^{13}C CP NMR.

Component		Stretching ×1.5	Ratio ×3.5
Case A			
1: well-oriented	α_{F1}	90	90
	β_{F1}	12	13
	p_1	13	13
	Fraction	0.15	0.30
2: poorly-oriented	α_{F2}	90	90
	β_{F2}	30	25
	p_2	22	18
	Fraction	0.22	0.17
3: amorphous fraction		0.63	0.53
Case B			
1: well-oriented	α_{F1}	90	90
	β_{F1}	5	6
	p_1	7	6
	Fraction	0.15	0.35
2: poorly-oriented	α_{F2}	90	90
	β_{F2}	17	16
	p_2	16	16
	Fraction	0.27	0.21
3: amorphous fraction		0.58	0.44

NMR analyses of the oriented component together with the values, β_F and p. The sum of the fractions of the well-oriented and poorly-oriented components for case B were larger than for case A and the oriented distribution (β_F and p) of case B is smaller than for case A. Therefore the entropy of case B with stretching ratio 3.5 was smaller and the T_m shifts to a higher temperature.

3.6. Conformational change of PGA molecules by stretching studied with MD simulations

The appearance of crystal structure with trans conformation in PGA samples by stretching could be monitored by X-ray diffraction and ^{13}C CP/MAS NMR. The change in the heterogeneous structures of PGA samples in view points of orientation was also clarified using ^{13}C CP NMR by changing the angle between the fiber axis and the magnetic field. However, it is difficult to monitor change in the other conformations by stretching experimentally. Therefore MD simulation was performed to study such a conformational change complementally.

At the initial structural model before stretching, the conformation of the bond, –O-C(=O)–, was trans. After MD simulation under stretching condition, the conformation of the bond was still trans. This seems due to partial double bond character of –O–C(=O)– bond. Thus, the conformational change by stretching occurs exclusively at other two bonds, –C(=O)–CH_2– and –CH_2–O– of the PGA molecules. Fig. 7 shows the conformational distributions of initial amorphous PGA model (×1.0) (a) and also the models stretched by ×1.34 (b) and ×1.80 (c) after MD simulations as an example. At the amorphous PGA model (Fig. 7 a), there are three conformations, *T*, *G* and *G′* around the –CH_2–O– bond and two conformations, *G* and *G′* around the –C(=O)–CH_2– bond although the conformational distribution is wide. The appearance of only two conformations for the –C(=O)–CH_2– bond is due to unstable trans conformation because of the repulsion between the O atom of C(=O) bond and backbone O atom of –CH_2–O– bond along the chain. By stretching (×1.34) (Fig. 7 b), there are still three conformations, *T*, *G* and *G′* around the –CH_2–O– bond. However, a small difference from Fig. 7 a was predicted, that is, the distribution around the trans conformation tends to be narrow. The

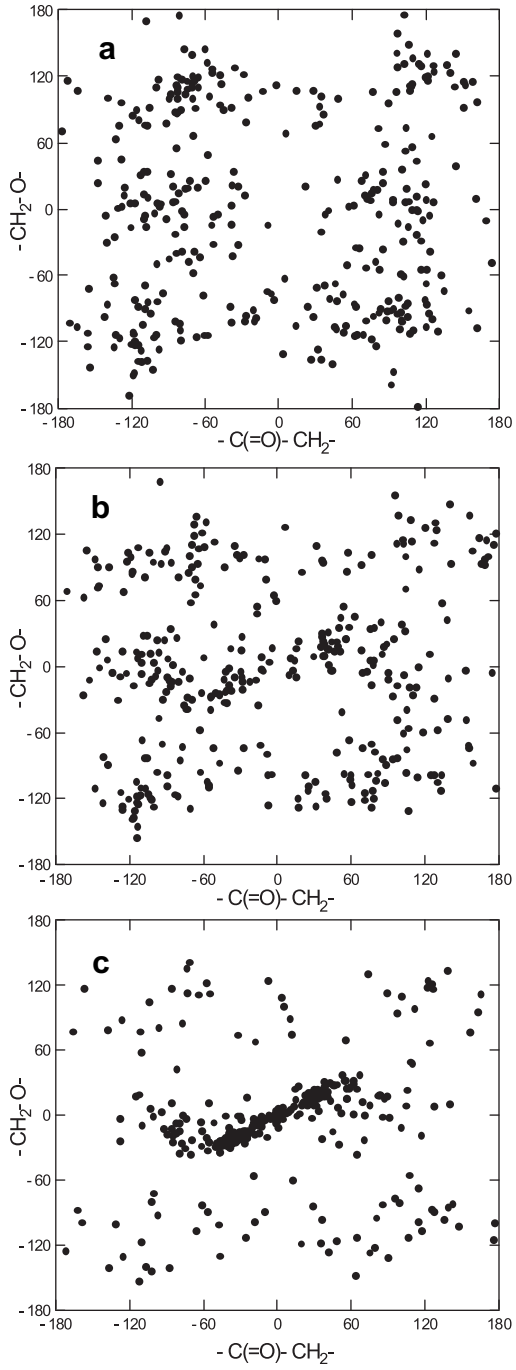

Fig. 7. Conformational distributions around two bonds, –C(=O)–CH_2– and –CH_2–O–, of PGA calculated with the stretching ratios, ×1.0 (a), ×1.34 (b) and ×1.80 (c) in the MD simulation.

conformation around trans –C(=O)–CH_2– bond newly appeared and therefore there are many conformations with the internal rotation angles from 0 to ±180 degree around the –C(=O)–CH_2– bond. By further stretching (×1.80) (Fig. 7 c), the conformations with both trans and trans forms for –CH_2–O– and –C(=O)–CH_2– bonds, respectively appeared although the deviation of the internal rotation angles is relatively large especially for the bond, –CH_2–O–. Thus, the generation of trans conformation for all three bonds by stretching was reproduced. The process of the conformational change could be monitored by the MD simulation. The domains of stretched PGA chains with trans conformation of around 0 degree

for three bonds seem to be well-oriented components in Fig. 6. On the other hand, the domains of stretched PGA chains with trans conformation of the internal rotation angles which are deviated from 0 degree largely around the bond, $-CH_2-O-$ in Fig. 7 c, might be poorly-oriented components in Fig. 6. Other conformations correspond to amorphous region and the fraction decreases with stretching.

4. Conclusion

It has been shown that the ^{13}C CP NMR spectra without MAS of the stretched PGA fibers observed by changing the angle between the fiber axis and magnetic field showed heterogeneous structures which consist of three components; well-oriented, poorly-oriented and isotropic amorphous components. Change in the heterogeneous structure, that is, appearance of trans conformation by stretching was monitored by X-ray diffraction and ^{13}C CP NMR experimentally. These analyses elucidate that the T_g and T_m shifts were caused by the oriented amorphous region, and the data supports the study of modulus and X-ray scattering study of De Oca et al. [9]. The MD simulation was performed to study such a conformational change complementally. The generation of trans conformation for all three bonds by stretching was reproduced by the simulation.

Acknowledgment

SS is grateful to Mr. H. Kanno, Ms. M. Koyama and S. Nakamura (Mitsui Chemical Analysis & Consulting Service, Inc.) for the X-ray diffraction and DSC measurements. TA acknowledges support in part by the Program for Promotion of Basic and Applied Researches for Innovations in Bio-oriented Industry and the Grant-in-Aid for Scientific Research from the Ministry of Education, Science, Culture and Sports of Japan (18105007). KY acknowledges the financial support of SENTAN JST for the probehead development.

References

[1] Gilding DK, Reed AM. Polymer 1979;20:1459.
[2] Blomqvist J, Mannfors B, Pietila LO. Polymer 2002;43:4571.
[3] Fu BX, Hsiao BS, Chen G, Zhou J, Koyfman I, Jamiolkowski DD, et al. Polymer 2002;43:5527.
[4] Nakafuku C, Yoshimura H. Polymer 2004;45:3583.
[5] Chu CC. J Appl Polym Sci 1981;26:1727.
[6] Chatani Y, Suehiro K, Okita Y, Tadokoro H, Chujo K. Makromol Chem 1968;113:215.
[7] Sobczak M, Chreptowicz T, Kolmas J, Kolodziejski W. Solid State Nucl Magn Reson 2009;35:230.
[8] Oca HM, Ward IM, Klein PG, Ries ME, Rose J, Farrar D. Polymer 2004;45:7261.
[9] Oca HM, Ward IM. Polymer 2006;47:7070.
[10] Sekine S, Akieda H, Ando I, Asakura T. Polym J 2008;40:10–6.
[11] Nicholson LK, Asakura T, Demura M, Cross TA. Biopolymers 1993;33:847.
[12] Asakura T, Minami M, Shimada R, Demura M, Osanai M, Fujito T, et al. Macromolecules 1997;30:2429.
[13] Demura M, Yamazaki Y, Asakura T, Ogawa K. J Mol Struct 1998;441:155.
[14] Demura M, Minami M, Asakura T, Cross TA. J Am Chem Soc 1998;120:1300.
[15] Asakura T, Ito T, Okudaira M, Kameda T. Macromolecules 1999;32:4940.
[16] Zhao CH, Asakura T. Prog NMR Spectrosc 2001;39:301.
[17] Asakura T, Konakazawa T, Demura M, Ito T, Maruhashi Y. Polymer 1996;37:1965.
[18] Ito T, Maruhashi Y, Demura M, Asakura T. Polymer 2000;41:859.
[19] Ito T, Yamaguchi Y, Watanabe H, Asakura T. J Appl Polym Sci 2001;80:2376.
[20] Chujo K, Kobayashi H, Suzuki J, Tokuhara S. Makromol Chem 1967;100:267.
[21] Zachmann HG. Kolloid Z Z Polym 1969;231:504.
[22] Wunderlich B. Polymer 1964;5:125.
[23] Todoki M, Kawaguchi T. J Polym Sci Polym Phys Ed 1977;15:1507.
[24] Todoki M. Thermochim Acta 1985;93:147.